Coherent Electronic Transport through Graphene Constrictions: Subwavelength Regime and Optical Analogy

Pierre Darancet, Valerio Olevano, and Didier Mayou

Institut Néel, CNRS and UJF, Grenoble, France and European Theoretical Spectroscopy Facility (ETSF), Grenoble, France

(Received 3 October 2008; published 31 March 2009)

Nanoelectronic devices smaller than the electron wavelength can be achieved in graphene with current lithography techniques. Here we show that the electronic quantum transport of graphene subwavelength nanodevices presents deep analogies with subwavelength optics. We introduce the concept of electronic diffraction barrier to represent the effect of constrictions and the rich transport phenomena of a variety of nanodevices. Results are presented for Bethe and Kirchhoff diffraction in graphene slits and Fabry-Perot interference oscillations in nanoribbons. The same concept applies to graphene quantum dots and gives new insight into recent experiments in these systems.

DOI: 10.1103/PhysRevLett.102.136803 PACS numbers: 73.63.−b, 42.25.Fx, 42.50.St, 72.10.Fk

Analogies play a prominent role in physics. They allow the transfer of notions and concepts from one field to another, thus providing deeper insights in both fields. In particular, analogies between quantum transport and optics have been suggested in the past. For instance, they have been used to better understand coherent multiple scattering of light [1], or reciprocally electronic transport as transmission of optical waves [2]. More recently, optical concepts have also been applied to analyze some electronic properties of graphene [3].

In this Letter, we develop the analogy between quantum transport and optics beyond those former attempts, and bridge coherent electronic transport with subwavelength optics. This is motivated by the exceptional electronic coherence of graphene [4,5], both in its exfoliated and epitaxial forms. The electron mean free path could ultimately reach the micrometer range at room temperature [6], and the electronic wavelength, close to the Dirac point, is larger than 100 nm in exfoliated graphene [6] and even larger than 500 nm in the lowest doped graphene layers [7] of epitaxial graphene. From a technological point of view, graphene can be patterned with standard or even STM [8] lithography techniques into devices as small as one or a few tens of nanometers, thus reaching the subwavelength regime.

We present results for simple systems, which have optical analogues [9–13], such as slits and nanoribbons connecting two graphene half-planes. We consider also quantum dots connected to semi-infinite graphene sheets. We perform an exact numerical calculation of the low-bias conductance within a tight-binding model [14] and Landauer quantum transport formalism [2]. The Landauer conductance can be computed by the standard principal layer approach [2], but we used a new recursive numerical algorithm [15] that we found more efficient. We introduce the concept of *electronic diffraction barrier* to represent the effect of constrictions at contacts. This provides a simple way to describe the rich phenomena of transport physics in a variety of subwavelength graphene nanodevices. Our results give new insights into the conductance characteristics of graphene quantum dots [16,17], where a chaotic Dirac billiard behavior has been recently observed [16]. We propose a new interpretation of quantum dot characteristics that we relate to the diffraction phenomena when the electronic wavelength diverges at the Dirac point.

Conductance of graphene slits and diffraction by an aperture—.We calculate the conductance of slits of various width W, in a graphene sheet (Fig. 1), the graphene half-planes having armchair edges. The thinnest slit consists of only a single *motif*, i.e., a single hexagon. The wavelength λ of the incident Dirac electrons is related to the energy E via $\lambda = h v_F / E$, where $v_F \simeq 10^6\ \mathrm{ms}^{-1}$ is the Fermi velocity.

In Fig. 1 we plot the low-bias conductance of the slits as a function of W/λ. We first notice (Fig. 1, inset) that the conductance depends only on the ratio W/λ, provided that the wavelength is $\lambda \lesssim 4$ nm, that is, for an energy $E \gtrsim 1$ eV. This scaling is related to the massless 2D Dirac

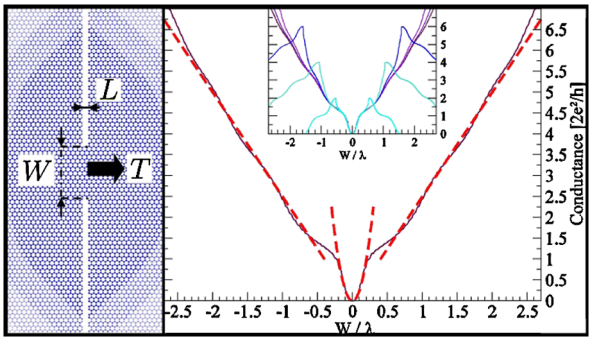

FIG. 1 (color online). Diffraction of electrons through a graphene slit. Left: Geometry of a graphene slit. Right: Universal scaling law of the low-bias conductance of the graphene slit as a function of W/λ. This shows the Bethe-like $\lambda \gg W$ quadratic regime and the Kirchhoff-like $\lambda \ll W$ linear regime (see text). The inset shows the conductance for slits of various widths $W \simeq 0.8p$ nm, with $p = 1, 2, 3, \ldots$.

equation, which is valid only in the low energy or long wavelength limit in graphene. If a spinor $\psi(r)$ satisfies the Dirac equation for the energy E and wavelength λ, then the spinor $\tilde{\psi}(r) = \psi(xr)$ satisfies the Dirac equation for the energy $\tilde{E} = E/x$ and wavelength $x\lambda$. Therefore, the conductance shows a scale invariance $g(x\lambda, xW) = g(\lambda, W)$. As a consequence, the conductance only depends on a reduced variable W/λ, $g(\lambda, W) = g(W/\lambda)$ [18]. Note that a scaling relation can also exist for other geometries. In that case, the conductance of the circuit will depend only on the ratio between the characteristic lengths of the circuit and the wavelength λ.

In the limit $W/\lambda \ll 1$, the low-bias conductance is quadratic, with the conductance $g(W/\lambda) \simeq 50(e^2/h) \times (W/\lambda)^2$, while in the opposite limit $W/\lambda \gg 1$, the conductance is linear with $g(W/\lambda) \simeq 5(e^2/h)(W/\lambda)$. The crossover between the two regimes occurs around $W/\lambda \simeq 0.2$–0.5. This is similar to the findings in classical optics and consequently offers an immediate interpretation: the conductance response of a graphene slit is a clear manifestation of a diffraction phenomenon. Indeed, we can identify two different diffraction regimes: for wavelengths $\lambda \gg W$, much larger than the aperture, we observe a Bethe-like diffraction regime [9] with a slit transmitted energy proportional to the square of the aperture. On the other hand, $\lambda \ll W$ corresponds to a Kirchhoff-like diffraction regime, where the transmitted energy is proportional to the aperture. In the short wavelength limit diffraction is a perturbation phenomenon and a semiclassical description of the electrons as ballistic wave packets is applicable. Consequently, the transmitted current is proportional to the section of the slit W and the conductance diverges for large slits. By contrast, in the subwavelength regime the transmission is lower than expected from the semiclassical picture and can be viewed as a coherent tunneling process.

Note that for narrow graphene ribbons somewhat similar ideas have also been proposed [5]. A decrease of the transmittance at the Dirac energy has also been obtained for constrictions on graphene nanoribbons [20]. Diffraction effects in the Kirchhoff regime could also arise at the lead mouth of quantum billards [21].

Nanoribbons as Fabry-Perot interferometers and subwavelength waveguides.—Here we study the quantum transport response of finite-length metallic graphene nanoribbons. We consider two metallic ribbons of zigzag and armchair orientation, respectively. Both have one conducting channel at the Dirac energy [22]. The geometry is presented in Fig. 2: the length of the armchair nanoribbon is 6 and 3 nm for the zigzag ribbon. The calculated conductance for both ribbons is shown in Fig. 2. Similarly to the slit geometry, we observe a zero conductance value at the Dirac point. However, in the ribbon case, another important feature is the large amplitude of the conductance *oscillations*.

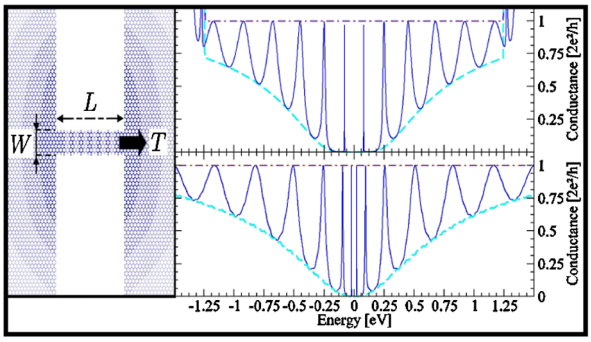

FIG. 2 (color online). Left: Schematic view of nanoribbons contacted to graphene half-planes. The exact geometry of the junction is presented in Fig. 3. Right: Fabry-Perot oscillations in the low-bias conductance of armchair (upper panel) and zigzag (lower panel) nanoribbons. The envelope of the conductance minima follows almost perfectly Eq. (2), which is plotted with a dashed curve for $R(E)$ taken from Fig. 3. See text.

We now demonstrate that these systems behave as Fabry-Perot cavities, like subwavelength optical metallic waveguides [11–13]. The Fabry-Perot oscillations are due to the reflection at the ends of the nanoribbons, and the low-bias conductance varies like the Fabry-Perot transmittance, which is the Airy function:

$$T_{\mathrm{FP}}(E) = \frac{1}{1 + F(E)\sin^2[\phi(E)/2]}, \tag{1}$$

where $\phi(E) = 2k(E)L + 2\tilde{\phi}(E)$ is the phase difference after one back and forth reflection at each end of the nanoribbon. $k(E)$ is the wave vector of the Bloch state in the infinite ribbon at the energy E. $\tilde{\phi}(E)$ is the phase factor acquired at each reflection. L is the length of the Fabry-Perot interferometer. $F(E) = 4R(E)/[1 - R(E)]^2$ is the *finesse* coefficient and $R(E) = 1 - T(E)$ is the reflection coefficient at each end of the nanoribbon, that is, at the ribbon–half-plane junction.

In accordance with our numerical results, the Airy function presents maxima $T_{\mathrm{FP}}^{\max} = 1$, when $\phi/2$ is an integer m multiple of π. For sufficiently large L the phase $\phi(E) = 2k(E)L + 2\tilde{\phi}(E)$ varies rapidly with energy, as compared to $F(E)$. The minima occur when $\sin^2(\phi/2)$ is maximum, that is, at $\phi/2 = m\pi + \pi/2$. The envelope of the minima follows the function

$$T_{\mathrm{FP}}^{\min}(E) = \frac{1}{1 + F(E)} = \frac{[1 - R(E)]^2}{[1 + R(E)]^2}. \tag{2}$$

In particular, Eq. (2) is independent of the ribbon length, which agrees with our numerical calculations on nanoribbons of various lengths (not shown here). More specifically, the minimum of the transmission tends to zero at the Dirac energy, which indicates that $R(E)$ tends to 1 at zero energy.

Another characteristic feature of the Fabry-Perot resonances is their width. The full width at half maximum of

the peaks is $\delta E_{\mathrm{FWHM}} = \delta\phi \frac{dE}{d\phi} = \delta\phi \frac{v(E)}{2L}$, where $\delta\phi = 2(1-R)/\sqrt{R}$ and $v(E)$ is the group velocity at energy E. For the armchair nanoribbon the velocity is finite, such that the peaks are narrow when R is close to 1, and broaden when $R \to 0$. In our conductance calculation, when $E \to 0$ the peaks have negligible width, which confirms that $R \to 1$. For zigzag nanoribbons both $v(E)$ and $T(E) = 1 - R(E)$ tend to zero at the Dirac energy and lead to fine peaks.

Fabry-Perot oscillations occur in many devices through which the electron wave is transmitted, in particular, in nanotubes or graphene devices [23]. Yet the reflection at the ends of the device is usually only partial, whereas in the present study the reflection is total at the Dirac point due to diffraction. Consequently, close to that point the conductance minima are nearly zero. Let us consider, as a simple criterion, that resonances are well defined if the maximum to minimum ratio of the conductance is greater than 2. In our calculations this corresponds to the condition $\lambda/W \gtrsim 3$–5, where W is the width of the nanoribbon.

Concept of electronic diffraction barrier at a constriction.—We now analyze the reflection at the end of the nanoribbon. For this, we consider the response of one elementary junction consisting of a graphene half-plane connected to a semi-infinite metallic zigzag or armchair ribbons (Fig. 3). For a ballistic system (infinite ribbon, no contact resistance and no reflection), the conductance would be equal to 1 quantum of conductance ($2e^2/h$) (dot-dashed line in Fig. 3). Instead, the calculated transmittance $T(E)$ through the junction (continuous line in Fig. 3) drops to zero at the Dirac energy, for both chiralities, exactly like in slits and nanoribbons. The only effect of the ribbon electronic structure is to produce a slight difference in the $T(E)$ characteristics, with the zigzag conductance showing a more cusplike feature at the Dirac energy. The transmittance of this elementary junction defines the characteristics of the elementary electronic diffraction barrier. The electronic diffraction barrier is at the basis of the universal behavior observed in all the devices studied here.

The resistance of the metallic ribbon is independent of its length and depends only on the incident wavelength (or energy), which is a genuine manifestation of the contact resistance at the junction. For instance, back to the nanoribbon case, we plot $[1-R(E)]^2/[1+R(E)]^2$ (dashed curve in Fig. 2) with $R(E) = 1 - T(E)$ extracted from Fig. 3 for the elementary junction. This curve turns out to be the envelope of the Fabry-Perot oscillations minima of the nanoribbon conductance, as expected from Eq. (2).

Conductance of a quantum dot.—We now turn to more complicated structures and consider a quantum dot (Fig. 4) consisting of a purposely irregular shape graphene nanostructure contacted via small apertures to the two half-planes graphene leads. We note that the conductance of this system (Fig. 4) presents a maximum around 3 eV, which is the energy of the van Hove singularity of bulk graphene where the density of states diverges. The maximum value of the conductance can increase indefinitely if the size of the dot and of its junction with the graphene plane increases. The conductance decreases when going to the Dirac point. This is a signature of the lower number of available states at the Dirac point. The maximum to minimum transmission ratio between adjacent peaks is much larger in the vicinity of the Dirac energy than at other energies. This is also observed in the nanoribbons studied above. Again this can be explained by the presence of two diffraction barriers at the contacts that are nearly completely reflecting ($R = 1$) at the Dirac energy. This leads to well-defined states within the quantum dot, and thus well-defined conduction channels through these states. The energy range with well-defined resonances can be identified with the same criterion as above, i.e., maximum to minimum ratio greater than 2. This criterion gives a critical wavelength of order of $\lambda \simeq 4$ nm for a width $W = 1.2$ nm. This is the same range of values of λ/W as in nanoribbons, i.e., $\lambda/W \gtrsim 3$–5.

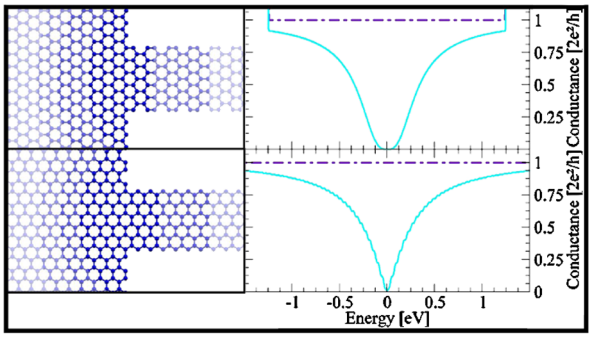

FIG. 3 (color online). Electronic diffraction barrier at a contact. Left: The contact geometries of the armchair (upper panel) and zigzag (lower panel) semi-infinite ribbons, having a width of five hexagons, coupled to graphene half-planes. Right: Conductance g for each device of the left panels. $g = 2e^2/hT$ with T the transmittance of the diffraction barrier.

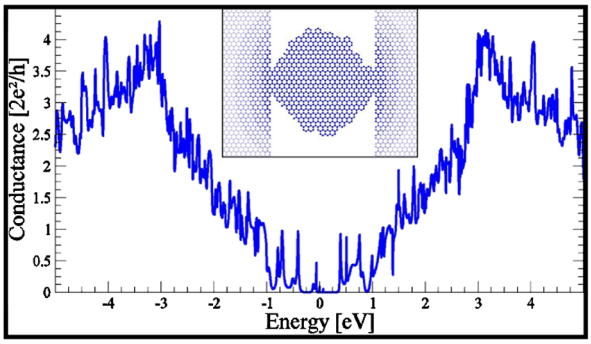

FIG. 4 (color online). Low-bias conductance of the quantum dot, showing well-defined resonances close to the Dirac energy. Inset: Geometry of the irregular shaped quantum dot coupled to the graphene half-planes.

Experimental consequences.—The computed characteristics of our quantum dot (Fig. 4) look quite similar to the experimental result of Ponomarenko *et al.* (Ref. [16], Fig. 1). In those experiments the electronic wavelength is $\lambda \simeq 130\ \mathrm{nm}/\sqrt{|V_g|}$ [24], where V_g is the gate voltage variation with respect to the Dirac point (in volts). In those experiments resonances are well defined for a wavelength λ to aperture W ratio $\lambda/W \gtrsim 3$–5 in reasonable agreement with our numerical estimate. Ponomarenko *et al.* also report the low-bias conductance of 20 nm constrictions (Ref. [16], Fig. S2), similar to the slits studied here. First of all, after our study of slits, the linear Kirchhoff-like regime is reached at voltages $V_g \geq 10$ V. For higher voltages we predict a conductance $g(W/\lambda) \simeq 5(e^2/h)(W/\lambda) \simeq 0.75(e^2/h)\sqrt{|V_g|}$ for a 20 nm slit. This is consistent with the experimental results. For instance, at $V_g = 100$ V we predict $G \simeq 7.5e^2/h$, in good agreement with the experimental value $G \simeq 5.5e^2/h$. On the other hand, the comparison of our results with the smaller 10 nm experimental constriction is not so good. Indeed there is evidence of thermally activated transport for the 10 nm constriction, which suggests a noncoherent transport mechanism.

To conclude, our work establishes an important link between nanoelectronics and subwavelength optics. We have developed the concept of electronic diffraction barrier which allows us to explain the conductance characteristics in terms of diffraction and interference phenomena for systems such as graphene junctions, slits, nanoribbons, and quantum dots. The deep analogy between quantum transport and optics that we have shown is a consequence of both the ondulatory nature of electrons and their linear dispersion in graphene, as for photons. Yet we believe that also for other dispersion relations, such as quadratic dispersion, similar effects can be observed as well. In particular, no matter the electronic structure, the ratio between the electronic wavelength and the characteristic size of the system remains a key parameter. We believe that the analogy developed here can be further pushed forward in the design of devices with new properties.

This work has benefited from many discussions. We thank, in particular, C. Berger, W. de Heer, L. Lévy, P. Mallet, C. Naud, K. Novoselov, T. Lopez-Rios, P. Quémerais, J. Y. Veuillen, and L. Wirtz.

[1] P.-E. Wolf and G. Maret, Phys. Rev. Lett. **55**, 2696 (1985).
[2] S. Datta, *Electronic Transport in Mesoscopic Systems* (Cambridge University Press, Cambridge, England, 1995).
[3] V. V. Cheianov, V. Fal'ko, and B. L. Altshuler, Science **315**, 1252 (2007).
[4] K. S. Novoselov *et al.*, Nature (London) **438**, 197 (2005); Y. Zhang, Y.-W. Tan, H. L. Stormer , and P. Kim, Nature (London) **438**, 201 (2005).
[5] C. Berger *et al.*, Science **312**, 1191 (2006); W. A. de Heer *et al.*, Solid State Commun. **143**, 92 (2007).
[6] K. I. Bolotin *et al.*, Solid State Commun. **146**, 351 (2008).
[7] M. Orlita *et al.*, Phys. Rev. Lett. **101**, 267601 (2008).
[8] L. Tapasztó, G. Dobrik, P. Lambin, L. P. Biró, Nature Nanotech. **3**, 397 (2008).
[9] H. A. Bethe, Phys. Rev. **66**, 163 (1944).
[10] T. W. Ebbesen *et al.*, Nature (London) **391**, 667 (1998); E. Ozbay, Science **311**, 189 (2006).
[11] P. Quémerais, A. Barbara, J. Le Perchec, and T. López-Rios, J. Appl. Phys. **97**, 053507 (2005); F. Ducastelle and P. Quémerais, Phys. Rev. Lett. **78**, 102 (1997); E. Belin and D. Mayou, Phys. Scr. **T49a**, 356 (1993); A. Pasturel, D. N. Manh, and D. Mayou, J. Phys. Chem. Solids **47**, 325 (1986).
[12] Y. Takakura, Phys. Rev. Lett. **86**, 5601 (2001).
[13] J. R. Suckling *et al.*, Phys. Rev. Lett. **92**, 147401 (2004).
[14] P. R. Wallace, Phys. Rev. **71**, 622 (1947).
[15] P. Darancet, V. Olevano, and D. Mayou arXiv:0903.0854v1; P. Darancet, Ph.D. thesis, University Joseph Fourier [http://tel.archives-ouvertes.fr/tel-00363630/fr/].
[16] L. A. Ponomarenko *et al.*, Science **320**, 356 (2008).
[17] C. Stampfer *et al.*, Appl. Phys. Lett. **92**, 012102 (2008).
[18] The argument is as follows. Let us consider a system where each half-plane of graphene is replaced by a ribbon of width $\tilde{W}$. The axis of symmetry of the ribbon is perpendicular to the slit, crossing through by the center of the slit. The conductance for a half-graphene plane is $g(\lambda, W) = \lim_{\tilde{W}\to\infty} g(\lambda, \tilde{W}, W)$. We consider a continuous type model for the graphene circuit [19]. In this model the mass term of the Dirac equation is zero in the graphene region and infinite outside. This confines the electrons in the graphene region. Then there is a one-to-one correspondence between the scattering states at wavelength λ, ribbon width $\tilde{W}$, slit width W and those at wavelength $x\lambda$, ribbon width $x\tilde{W}$, and slit width xW. This means that the conductance satisfies $g(\lambda, \tilde{W}, W) = g(x\lambda, x\tilde{W}, xW)$; therefore, $g(x\lambda, xW) = g(\lambda, W)$.
[19] N. M. R. Peres, A. H. Castro Neto, and F. Guinea, Phys. Rev. B **73**, 241403(R) (2006).
[20] F. Muñoz-Rojas, D. Jacob, J. Fernández-Rossier, and J. J. Palacios, Phys. Rev. B **74**, 195417 (2006).
[21] I. Brezinova, C. Stampfer, L. Wirtz, S. Rotter, and J. Burgdörfer, Phys. Rev. B **77**, 165321 (2008).
[22] K. Nakada, M. Fujita, G. Dresselhaus, and M. S. Dresselhaus, Phys. Rev. B **54**, 17 954 (1996).
[23] W. Liang *et al.*, Nature (London) **411**, 665 (2001); S. Cho, Y. F.Chen, and M. S. Fuhrer, Appl. Phys. Lett. **91**, 123105 (2007); J. P. Robinson and H. Schomerus, Phys. Rev. B **76**, 115430 (2007); A. V. Shytov, M. S.Rudner, and L. S. Levitov, Phys. Rev. Lett. **101**, 156804 (2008).
[24] K. S. Novoselov (private communication).